

Guaranteed Coverage Prediction Intervals with Gaussian Process Regression

Harris Papadopoulos

Abstract—Gaussian Process Regression (GPR) is a popular regression method, which unlike most Machine Learning techniques, provides estimates of uncertainty for its predictions. These uncertainty estimates however, are based on the assumption that the model is well-specified, an assumption that is violated in most practical applications, since the required knowledge is rarely available. As a result, the produced uncertainty estimates can become very misleading; for example the prediction intervals (PIs) produced for the 95% confidence level may cover much less than 95% of the true labels. To address this issue, this paper introduces an extension of GPR based on a Machine Learning framework called, Conformal Prediction (CP). This extension guarantees the production of PIs with the required coverage even when the model is completely misspecified. The proposed approach combines the advantages of GPR with the valid coverage guarantee of CP, while the performed experimental results demonstrate its superiority over existing methods.

Index Terms—Gaussian Process Regression, Conformal Prediction, Prediction Regions, Uncertainty Quantification, Coverage Guarantee, Normalized Nonconformity



1 INTRODUCTION

THE provision of confidence information about the predictions of Machine Learning techniques is highly desirable in many practical applications, especially in safety-critical areas such as learning-based robotics and control [1], [2], autonomous driving [3], estimating safe operating regions for reinforcement learning [4] and medical decision support [5]. Despite their importance, there are very few Machine Learning techniques that provide some kind of confidence information.

One such technique, which is becoming increasingly popular among the Machine Learning community, is Gaussian Process Regression (GPR) [6]. Due to its Bayesian probabilistic formulation, GPR produces a predictive distribution for each test instance rather than a plain point prediction. In addition, it has many other desirable properties, such as its nonparametric nature, the use of covariance functions that can be developed according to the data and problem in question, and the ability of using standard Bayesian methods for model selection.

There is however an important drawback of the predictive distributions produced by GPR. They rely on the assumption of the model being well-specified. As a result, in the case of model misspecification (e.g. wrong GP model hyperparameters or likelihood) these predictive distributions can become very misleading. For this reason, a number of recent works, such as [7]–[10], have attempted to derive more reliable uncertainty bounds for GPR by scaling the posterior standard deviation produced for each instance. These however, still cannot guarantee the required coverage in all cases of model misspecification.

This work addresses this problem by proposing an extension of the GPR approach that is guaranteed to produce well-calibrated prediction intervals (PIs) without assuming anything more than exchangeability of the data (exchangeability is a slightly weaker assumption than i.i.d.). The proposed approach is based on a Machine Learning framework, called Conformal Prediction (CP) [11], that can be combined with an underlying technique for producing prediction regions with a provably valid coverage of $1 - \delta$, for any significance level δ .

The main building block of CP is a real-valued function, called *nonconformity measure*, that evaluates how strange or nonconforming a candidate instance is from a set of known instances according to the underlying technique. In many cases it is possible to define more than one nonconformity measure for a given underlying algorithm and each one defines a different Conformal Predictor. An important attractive property of CP is that the nonconformity measure definition and underlying algorithm of a particular Conformal Predictor have no effect on its coverage guarantee, they only affect its statistical efficiency i.e. the sizes of the resulting prediction regions.

The CP framework has two main versions: Transductive CP (TCP), also known as Full CP, and Inductive CP (ICP), also referred to as Split CP. The former utilizes all available data for both training the underlying method and calibrating its prediction regions, while the latter divides the data into distinct training and calibration sets. As a result, TCP achieves higher statistical efficiency at the cost of increased computational demands, while ICP maintains the computational efficiency of the algorithm it is based on, but sacrifices some statistical efficiency. Additionally, there is the Cross-Conformal Prediction (CCP) version of the framework, which combines the ideas of ICP and cross-validation. CCP falls somewhere in between TCP and ICP in terms of statistical and computational efficiency. However, it is important to note that CCP does not enjoy the theoretical

H. Papadopoulos is with the Department of Electrical Engineering, Computer Engineering and Informatics, Frederick University, Nicosia 1036, Cyprus.
E-mail: h.papadopoulos@frederick.ac.cy
Manuscript received November 25, 2022; revised October 18, 2023 and March 5, 2024; accepted June 7, 2024.
Digital Object Identifier 10.1109/TPAMI.2024.3418214

validity of the other two versions.

The application of ICP to some conventional technique is rather trivial; a recent overview of the process can be found in [12]. The same goes for CCP [13]. On the contrary, in the case of regression the application of TCP is only possible if some computational trick can be employed in order to allow efficient calculation of the CP prediction intervals. As a result, TCP has only been applied to Ridge Regression [14], the Lasso [15] and k -Nearest Neighbours Regression [16], [17]. The latter also introduced the concept of *normalized nonconformity measures* for regression CP, which result in improved statistical efficiency by taking into consideration the difficulty of the particular instance for the underlying technique. Since their introduction in [16], normalized nonconformity measures have become the standard for regression ICPs, but so far they have been employed in only one TCP (the k -Nearest Neighbours Regression TCP).

This paper proposes an algorithm for efficiently computing the PIs of TCP with a GPR underlying model. The proposed method combines the desirable properties of GPR with the *model-free* coverage guarantee of CP. Furthermore, unlike all previously proposed TCPs apart from k -Nearest Neighbours Regression, it utilizes a normalized nonconformity measure definition based on the predictive variance produced by GPR, leading to more accurate PIs.

The remainder of this paper is structured as follows. Section 2 introduces the Conformal Prediction framework and provides an overview of relevant work. Following this, Section 3 develops two efficient versions of the transductive GPR Conformal Predictor (GPR-CP). One of these versions is further enhanced in Section 4 with the introduction of a normalized nonconformity measure based on the predictive variance produced by GPR. Section 5 presents an experimental evaluation of the proposed method on both simulated and benchmark data sets, along with comparisons to other approaches. Finally, Section 6 offers concluding remarks and outlines future directions.

2 BACKGROUND

2.1 Conformal Prediction

Given a training set¹ of l observations $\{z_i\}_{i=1}^l$, where each $z_i \in \mathcal{Z}$ is a pair (x_i, y_i) consisting of the vector $x_i \in \mathcal{X}$ of inputs or features for case i and the associated output or label $y_i \in \mathbb{R}$ (dependent variable). Additionally, the inputs for a new observation x_{l+1} are provided and the objective is to produce a prediction region that will cover the correct output y_{l+1} with a predefined coverage rate of $1 - \delta$. As mentioned in Section 1, the only assumption made is that all (x_i, y_i) , $i = 1, 2, \dots$, are exchangeable.

CP considers every candidate value $\tilde{y} \in \mathbb{R}$ and uses the nonconformity measure to assign a value $\alpha_i^{\tilde{y}}$ to each instance z_i in the extended set

$$Z^{\tilde{y}} = \{z_1, \dots, z_l, z_{l+1}^{\tilde{y}}\}, \quad (1)$$

where $z_{l+1}^{\tilde{y}} = (x_{l+1}, \tilde{y})$. Formally, a nonconformity measure is a measurable mapping $A : \mathcal{Z}^{(*)} \times \mathcal{Z} \rightarrow \mathbb{R}$ (where $\mathcal{Z}^{(*)}$

is the set of all multisets of observations), which assigns a numerical score

$$\alpha_i^{\tilde{y}} = A(Z_{-i}^{\tilde{y}}, z_i) \quad (2)$$

to each $z_i \in Z^{\tilde{y}}$, where $Z_{-i}^{\tilde{y}}$ is the set resulting by the removal of z_i from $Z^{\tilde{y}}$. The value $\alpha_i^{\tilde{y}}$, called the *nonconformity score* of z_i , indicates how strange or nonconforming the pair (x_i, y_i) seems in relation to the instances in $Z_{-i}^{\tilde{y}}$. Note that $Z_{-i}^{\tilde{y}}$ is provided to A as an unordered set.

Typically each nonconformity measure is based on some conventional Machine Learning method called the *underlying algorithm* of the corresponding CP. Given a training set such as $Z^{\tilde{y}}$ each such method generates a prediction rule $D^{Z^{\tilde{y}}}$ that maps any unlabeled observation x_i to a predicted label $D^{Z^{\tilde{y}}}(x_i)$. As this prediction rule is based on the instances in $Z^{\tilde{y}}$, a natural measure of the nonconformity of each observation $z_i \in Z^{\tilde{y}}$ is the degree of disagreement between the predicted label

$$\hat{y}_i = D^{Z^{\tilde{y}}}(x_i) \quad (3)$$

and y_i for $i = 1, \dots, l$ or \tilde{y} for $i = l + 1$. The simplest way of measuring the disagreement of y_i and \hat{y}_i is by the absolute value of their difference $|y_i - \hat{y}_i|$.

Note that in (3) z_i is included in the training set of the underlying algorithm. Alternatively, we can generate the prediction rule $D^{Z_{-i}^{\tilde{y}}}$ by using $Z_{-i}^{\tilde{y}}$ as training set, and measure nonconformity as the degree of disagreement between the leave-one-out predicted label

$$\hat{\tilde{y}}_i = D^{Z_{-i}^{\tilde{y}}}(x_i) \quad (4)$$

and y_i for $i = 1, \dots, l$ or \tilde{y} for $i = l + 1$. Section 3 will consider both these cases with Gaussian Process Regression as underlying algorithm.

The nonconformity scores $\{\alpha_i^{\tilde{y}}\}_{i=1}^{l+1}$ of all instances in $Z^{\tilde{y}}$ can then be used to calculate the p -value of the null hypothesis that $\tilde{y} = y_{l+1}$ as

$$p(Z^{\tilde{y}}) = \frac{|\{i = 1, \dots, l + 1 : \alpha_i^{\tilde{y}} \geq \alpha_{l+1}^{\tilde{y}}\}|}{l + 1}, \quad (5)$$

also denoted as $p(\tilde{y})$.

To show why $p(\tilde{y})$ provides a valid p -value for testing the null hypothesis that $\tilde{y} = y_{l+1}$, note that the exchangeability assumption implies a uniform distribution over all permutations of z_1, \dots, z_{l+1} . Consequently, when $\tilde{y} = y_{l+1}$, the distribution over all permutations of $\alpha_1^{y_{l+1}}, \dots, \alpha_{l+1}^{y_{l+1}}$ is also uniform, and as a result, if all $\alpha_i^{y_{l+1}}$, $i = 1, \dots, l + 1$ are distinct $p(y_{l+1})$ is uniformly distributed over the set $\{1/(l + 1), 2/(l + 1), \dots, 1\}$. Therefore, since any equality $\alpha_i^{y_{l+1}} = \alpha_j^{y_{l+1}}$ for any i and j can only result in increasing $p(y_{l+1})$, for any significance level $\delta \in [0, 1]$,

$$\mathbb{P}\left((l + 1)p(y_{l+1}) \leq \delta(l + 1)\right) \leq \delta. \quad (6)$$

Based on (6), given a significance level δ , a regression Conformal Predictor generates the prediction region,

$$\mathcal{C}^\delta(x_{l+1}) = \{\tilde{y} : p(\tilde{y}) > \delta\}, \quad (7)$$

which has a valid finite-sample coverage. This is stated in the following theorem.

1. The training set is in fact a multiset as it can contain some observations more than once.

Theorem 1. (Conformal Prediction coverage guarantee [11]).

Suppose $(x_1, y_1), \dots, (x_{l+1}, y_{l+1})$ are exchangeable, then the Conformal Prediction region (7) satisfies

$$\mathbb{P}(y_{l+1} \in \mathcal{C}^\delta(x_{l+1})) \geq 1 - \delta.$$

The proof comes directly from the definition of the CP prediction region (7) and the property (6) of the p-value function (5).

Notice that the full CP framework, described here, treats both the training and the test instances in the same manner for calculating the p-value $p(\tilde{y})$ for each candidate label \tilde{y} . Specifically, it calculates the nonconformity scores $\{\alpha_i^{\tilde{y}}\}_{i=1}^{l+1}$ by incorporating the assumed pair (x_{l+1}, \tilde{y}) into the training set, thus applying distinct prediction rules for each \tilde{y} . This is critical for ensuring a uniform distribution over all permutations of $\alpha_1^{y_{l+1}}, \dots, \alpha_{l+1}^{y_{l+1}}$, leading to a valid finite-sample coverage. In the absence of this equal treatment, the nonconformity scores of the training instances would often be biased downwards, resulting in prediction regions that grossly undercover.

Of course it would be impossible to explicitly consider every possible output $\tilde{y} \in \mathbb{R}$. Section 3 describes how we can compute the prediction region (7) efficiently with Gaussian Process Regression as underlying algorithm.

2.2 Related Work

CP was first developed as a transductive classification approach for Support Vector Machines in [18] and later greatly improved in [19]. Soon it started being combined with several popular classifiers, such as k -Nearest Neighbours [20], [21], Neural Networks [22], Decision Trees [23], Random Forests [24] and Evolutionary Classifiers [25]. In all cases the developed methods were shown to produce well-calibrated and useful in practice confidence measures.

In the case of regression, which is the focus of this work, a computationally efficient transductive Ridge Regression CP was proposed in [14]. This work used the absolute values of the underlying model residuals as nonconformity measure. Various versions of k -Nearest Neighbours Regression TCP and ICP along with the concept of normalized nonconformity measures were proposed in [16], [17]. Normalized nonconformity measures divide the standard regression measure (the absolute values of the underlying model residuals) with a measure of the difficulty of each instance for the underlying model, thus resulting in more precise PIs. The nonconformity measures proposed in [17] used the distance of the k -nearest neighbours and the standard deviation of their labels as difficulty measures. The transductive version of the framework was also applied to the Lasso in [15], with only the standard non-normalized measure however.

As opposed to the transductive form of the framework, where normalized nonconformity measures have only been developed for k -Nearest Neighbours Regression, in the inductive form of the framework various normalized nonconformity measures have been developed for other popular regression techniques such as Ridge Regression [26], Neural Networks Regression [27] and Regression Forests [28], [29]. The normalized measures used in these works assess the

difficulty of each instance as: (1) the predictions of a separate linear model trained on the residuals of the original underlying model [26]–[28]; (2) the average error of the k -nearest neighbours of the instance [28]; (3) the variance of the predictions of individual ensemble members [29]. A recent study [30] investigates the effect of different underlying techniques, difficulty measures, and their parameters, on the performance of normalized inductive conformal regressors with random forest and gradient boosting.

CP has attracted a lot of attention in application areas where the reliable quantification of uncertainty is important, such as ovarian cancer detection [31], stroke risk assessment [32], drug discovery [33], bioactivity modeling [34], electricity price forecasting [35], software effort estimation [36] and text classification [37]. It has also been extended to additional problem settings such as multi-label learning [38], [39], multi-target regression [40], change detection in data streams [41], concept drift detection [42], anomaly detection [43] and active learning [44]. An extensive list of works and resources on CP can be found at [45].

A related approach to CP is the *jackknife prediction*, which defines PIs using the quantiles of leave-one-out residuals. However, the jackknife method does not provide any theoretical guarantees and in fact can have extremely poor coverage in some cases [46]. This was recently addressed with the introduction of *jackknife+* in [46], which like CP provides coverage guarantees under the assumption of exchangeability. Unlike CP though, *jackknife+* provides a guaranteed coverage rate of $1 - 2\delta$ (instead of $1 - \delta$). Furthermore, as opposed to CP with normalized nonconformity measures and therefore the approach proposed in this work, *jackknife+* does not provide any way of taking into consideration the difficulty of each instance for the underlying model, which results in more precise and informative PIs.

An alternative direction to uncertainty quantification for regression involves the provision of probability distributions instead of PIs through post-hoc model calibration [47]–[49]. Probability distributions offer the advantage of conveying richer information compared to PIs and can be readily transformed into PIs for any desired significance level. An extension of the CP framework for producing predictive distributions that are guaranteed to be calibrated in probability, named Conformal Predictive Systems (CPS), was developed in [50]. This approach was extended in [51] to Inductive CPS that can calibrate any model for producing fully adaptive to the test object predictive distributions.

Recalibration techniques however, including Inductive CPS, have a significant drawback compared to TCP. Achieving well-calibrated probability distributions necessitates setting aside a substantial portion of the available data for the calibration step, similarly to ICPs. This results in reduced statistical efficiency or even in some cases poor calibration when the data is limited.

Unlike recalibration techniques and ICPs, the approach developed in this paper utilizes the entire data set for both training the underlying model and calibrating the generated PIs, resulting in higher statistical efficiency. Furthermore, it combines the attractive properties of GPR, with the coverage guarantee of TCP and the precise PIs of a normalized nonconformity measure. Notably, it is the second TCP to incorporate a normalized measure.

3 GAUSSIAN PROCESS REGRESSION CP

This section begins with a brief overview of Gaussian Process Regression (GPR). A detailed introduction to all aspects of GPR can be found in [6]. GPR assumes that each output y_i is generated as $y_i = f(x_i) + \epsilon$, where ϵ is additive observational noise that follows a Gaussian distribution $\mathcal{N}(\epsilon|0, \sigma_n^2)$ and f is drawn from a Gaussian Process on the input space \mathcal{X} with covariance function $k : \mathcal{X} \times \mathcal{X} \rightarrow \mathbb{R}$ and mean $\mu : \mathcal{X} \rightarrow \mathbb{R}$. This in effect means that the joint distribution of any collection of function values $\mathbf{f} = (f(x_1), \dots, f(x_l))$ associated with the inputs $\mathbf{X} = (x_1, \dots, x_l)$ is multivariate Gaussian

$$p(\mathbf{f}|\mathbf{X}) = \mathcal{N}(\mathbf{f}|\mu, K), \quad (8)$$

where K is an $l \times l$ covariance matrix; in particular $K_{i,j} = k(x_i, x_j)$. For notational simplicity the mean function will be set to zero for the remainder of the paper.

The conditional distribution of a function value $f(x_{l+1})$ given the test input x_{l+1} and the training observations $\{z_i\}_{i=1}^l$ is also Gaussian with mean and variance

$$\hat{y}_{l+1} = \mathbf{k}_{l+1}^\top (K + \sigma_n^2 I)^{-1} \mathbf{y}, \quad (9a)$$

$$\sigma_{l+1}^2 = k(x_{l+1}, x_{l+1}) - \mathbf{k}_{l+1}^\top (K + \sigma_n^2 I)^{-1} \mathbf{k}_{l+1}, \quad (9b)$$

where \mathbf{k}_{l+1} is the vector of covariances between x_{l+1} and the l the training inputs, $\mathbf{y} = (y_1, \dots, y_l)^\top$ is the vector of observed outputs and I is the identity matrix. The predictive distribution for the test output y_{l+1} can be obtained by adding the noise variance σ_n^2 to (9b).

The corresponding expressions for the leave-one-out cross-validation predictive mean and variance (see [6], equation (5.12)) for an observation i are:

$$\hat{y}_i = y_i - \frac{[(K + \sigma_n^2 I)^{-1} \mathbf{y}]_i}{[(K + \sigma_n^2 I)^{-1}]_{ii}}, \quad (10a)$$

$$\hat{\sigma}_i^2 = \frac{1}{[(K + \sigma_n^2 I)^{-1}]_{ii}}, \quad (10b)$$

where $[\mathbf{v}]_i$ is the i th element of the vector \mathbf{v} and $[M]_{ii}$ is the i th diagonal element of the matrix M . Although this is used in [6] for model selection, it is particularly convenient for the construction of GPR-CP with $Z_{-i}^{\tilde{y}}$ as training set for measuring the nonconformity of each $z_i \in Z^{\tilde{y}}$ (see (4)).

The rest of this section develops a Conformal Predictor with GPR as underlying algorithm. As discussed in Section 2.1, every CP is based on a nonconformity measure, which assigns a score $\alpha_i^{\tilde{y}}$ to every observation $z_i \in Z^{\tilde{y}}$ (see (1)). This score quantifies the degree of disagreement between the observed label y_i and the predicted value \hat{y}_i (3) or $\hat{\tilde{y}}_i$ (4). The obvious nonconformity measure in the context of regression is

$$\alpha_i = |y_i - \hat{y}_i|, \quad (11)$$

when the underlying algorithm is trained on the whole set $Z^{\tilde{y}}$ and

$$\alpha_i = |y_i - \hat{\tilde{y}}_i|, \quad (12)$$

when the set $Z_{-i}^{\tilde{y}}$ is used as training set of underlying algorithm. This measure can also be enhanced by normalizing it with the difficulty of each input for the particular underlying technique [17]. One such measure is defined in the next Section.

Lets first consider the nonconformity measure (11). By replacing \hat{y}_i with the GPR mean (9a), the vector of nonconformity scores $|\mathbf{y} - \hat{\mathbf{y}}| = (\alpha_1, \dots, \alpha_{l+1})^\top$ can be written in the form

$$\begin{aligned} |\mathbf{y} - \hat{\mathbf{y}}| &= |\mathbf{y} - K(K + \sigma_n^2 I)^{-1} \mathbf{y}| \\ &= |(I - K(K + \sigma_n^2 I)^{-1}) \mathbf{y}| \\ &= |\sigma_n^2 (K + \sigma_n^2 I)^{-1} \mathbf{y}|. \end{aligned}$$

Since $\mathbf{y} = (y_1, \dots, y_l, 0)^\top + (0, \dots, 0, \tilde{y})^\top$, the vector of nonconformity scores can be represented as $|\mathbf{a} + \mathbf{b}\tilde{y}|$, where

$$\mathbf{a} = \sigma_n^2 (K + \sigma_n^2 I)^{-1} (y_1, \dots, y_l, 0)^\top, \quad (13a)$$

$$\mathbf{b} = \sigma_n^2 (K + \sigma_n^2 I)^{-1} (0, \dots, 0, 1)^\top. \quad (13b)$$

As a result, the nonconformity score $\alpha_i = \alpha_i(\tilde{y})$ of each observation $i = 1, \dots, l+1$ is a piecewise-linear function of \tilde{y} . Therefore, as the value of \tilde{y} changes, the p-value $p(\tilde{y})$ (defined by (5)) can only change at the points where $\alpha_i(\tilde{y}) = \alpha_{l+1}(\tilde{y})$ for some $i = 1, \dots, l$. This means that instead of having to calculate the p-value of every possible $\tilde{y} \in \mathbb{R}$, we can calculate the p-values of the finite number of points where $\alpha_i(\tilde{y}) = \alpha_{l+1}(\tilde{y})$ and of the intervals between them, leading to a feasible prediction algorithm [14].

Before going into the details of the algorithm lets first perform the same transformation with (12) as nonconformity measure. In effect this corresponds to $\hat{\tilde{y}}_i$ being the leave-one-out cross-validation predictions of GPR (10a) and therefore the vector of nonconformity scores $|\mathbf{y} - \hat{\tilde{\mathbf{y}}}| = (\alpha_1, \dots, \alpha_{l+1})^\top$ can be written in the form

$$\begin{aligned} |\mathbf{y} - \hat{\tilde{\mathbf{y}}}| &= |\mathbf{y} - \mathbf{y} + (K + \sigma_n^2 I)^{-1} \mathbf{y} / \text{diag}((K + \sigma_n^2 I)^{-1})| \\ &= |(K + \sigma_n^2 I)^{-1} \mathbf{y} / \text{diag}((K + \sigma_n^2 I)^{-1})|, \end{aligned}$$

where $\text{diag}(M)$ is a vector containing the diagonal elements of matrix M and $\mathbf{u}./\mathbf{v}$ is the element-by-element division of the vectors \mathbf{u} and \mathbf{v} . As a result, the vector of nonconformity scores can be represented as $|\mathbf{a} + \mathbf{b}\tilde{y}|$, where

$$\mathbf{a} = (K + \sigma_n^2 I)^{-1} \mathbf{y}_{\mathbf{a}} / \text{diag}((K + \sigma_n^2 I)^{-1}), \quad (14a)$$

$$\mathbf{b} = (K + \sigma_n^2 I)^{-1} \mathbf{y}_{\mathbf{b}} / \text{diag}((K + \sigma_n^2 I)^{-1}), \quad (14b)$$

$\mathbf{y}_{\mathbf{a}} = (y_1, \dots, y_n, 0)^\top$ and $\mathbf{y}_{\mathbf{b}} = (0, \dots, 0, 1)^\top$.

Using the vectors \mathbf{a} and \mathbf{b} from (13) or (14) it is now possible to efficiently calculate the set of output values \tilde{y} for which $p(\tilde{y}) > \delta$ for any given significance level δ . For each $i = 1, \dots, l+1$, let

$$\begin{aligned} S_i &= \{\tilde{y} : \alpha_i(\tilde{y}) \geq \alpha_{l+1}(\tilde{y})\} \\ &= \{\tilde{y} : |a_i + b_i \tilde{y}| \geq |a_{l+1} + b_{l+1} \tilde{y}|\}. \end{aligned} \quad (15)$$

Each set S_i (always closed) will either be an interval, a ray, the union of two rays, the real line, or empty; it can also be a point, which is a special case of an interval. As we are interested in the absolute values $|a_i + b_i \tilde{y}|$ we can assume that $b_i \geq 0$ for $i = 1, \dots, l+1$ (if not we multiply both a_i and b_i by -1). If $b_i \neq b_{l+1}$, then $\alpha_i(\tilde{y})$ and $\alpha_{l+1}(\tilde{y})$ are equal at two points (which may coincide):

$$-\frac{a_i - a_{l+1}}{b_i - b_{l+1}} \quad \text{and} \quad -\frac{a_i + a_{l+1}}{b_i + b_{l+1}}; \quad (16)$$

Algorithm 1 GPR-CP.

Input: training set $\{z_1, \dots, z_l\}$, new input x_{l+1} , covariance function k , vector of hyperparameters θ and significance level δ .

Calculate **a** and **b** as defined by (13) or (14)

$P \leftarrow \{\}$

for $i = 1$ to $l + 1$ **do**

if $b_i < 0$ **then**

$a_i \leftarrow -a_i$

$b_i \leftarrow -b_i$

end if

if $b_i \neq b_{l+1}$ **then**

 Add (16) to P ;

else if $b_i = b_{l+1} \neq 0$ **and** $a_i \neq a_{l+1}$ **then**

 Add (17) to P

end if

end for

Sort P in ascending order obtaining $y_{(1)}, \dots, y_{(u)}$

Add $y_{(0)} \leftarrow -\infty$ and $y_{(u+1)} \leftarrow \infty$ to P

$N(j) \leftarrow 0, j = 0, \dots, u$

$M(j) \leftarrow 0, j = 1, \dots, u$

for $i = 1$ to $l + 1$ **do**

$N(j) \leftarrow N(j) + 1, j = 0, \dots, u : (y_{(j)}, y_{(j+1)}) \in S_i$

$M(j) \leftarrow M(j) + 1, j = 1, \dots, u : y_{(j)} \in S_i$

end for

return the prediction region

$$\mathcal{C}^\delta(x_{l+1}) = \left(\bigcup_{j: \frac{N(j)}{l+1} > \delta} (y_{(j)}, y_{(j+1)}) \right) \cup \{y_{(j)} : \frac{M(j)}{l+1} > \delta\}.$$

in this case S_i is an interval (maybe a point) or the union of two rays. If $b_i = b_{l+1} \neq 0$, then $\alpha_i(\tilde{y}) = \alpha_{l+1}(\tilde{y})$ at just one point:

$$-\frac{a_i + a_{l+1}}{2b_i}, \quad (17)$$

and S_i is a ray, unless $a_i = a_{l+1}$ in which case S_i is the real line. If $b_i = b_{l+1} = 0$, then S_i is either empty or the real line.

To calculate the p-value $p(\tilde{y})$ for any potential output \tilde{y} of the new input x_{l+1} , we count how many S_i include \tilde{y} and divide by $l + 1$,

$$p(\tilde{y}) = \frac{\#\{i = 1, \dots, l + 1 : \tilde{y} \in S_i\}}{l + 1}. \quad (18)$$

As \tilde{y} changes value, $p(\tilde{y})$ can only change at the points (16) and (17), so for any significance level δ we can find the set of \tilde{y} for which $p(\tilde{y}) > \delta$ as the union of finitely many intervals and rays. Algorithm 1 implements a slightly modified version of this idea. It creates a list of the points (16) and (17), sorts it in ascending order obtaining $y_{(1)}, \dots, y_{(u)}$ and adds $y_{(0)} = -\infty$ to the beginning and $y_{(u+1)} = \infty$ to the end of this list. It then computes $N(j)$, the number of S_i containing the interval $(y_{(j)}, y_{(j+1)})$, for $j = 0, \dots, u$, and $M(j)$ the number of S_i containing the point $y_{(j)}$, for $j = 1, \dots, u$. Figure 1 illustrates the correspondence of the elements of N and M to these intervals and points.

Remark 1. The prediction region $\mathcal{C}^\delta(x_{l+1})$ produced by Algorithm 1 may not necessarily form a continuous interval as it may contain ‘holes’ within it. In practice, such cases are extremely rare; indeed, they were not

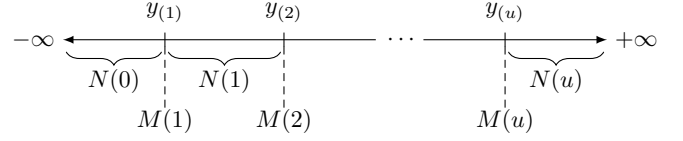


Fig. 1. Correspondence of N and M to the intervals and points of P .

observed in any experiments conducted as part of this study. However, to ensure the consistent production of PIs, Algorithm 1 can be adapted to output the convex hull of $\mathcal{C}^\delta(x_{l+1})$.

4 A NORMALIZED NONCONFORMITY MEASURE

Normalized nonconformity measures [17] divide the typical regression nonconformity with a measure of the difficulty of the particular input for the underlying algorithm. The intuition behind this is that two observations with the same nonconformity score as defined by (11) or (12), are not equally nonconforming if one of them is more difficult for the underlying algorithm. This differentiation is based on the expectation that the more difficult observation is likely to have a less accurate prediction, and therefore, it should be considered less nonconforming than the other, since their prediction accuracy is equal. Consequently, normalized nonconformity measures result in more precise PIs, which are tighter for inputs that are easier to predict and wider for inputs that are more difficult to predict.

In the case of Gaussian Process Regression, a readily available measure of the difficulty of an input x_i is its predictive variance $\hat{\sigma}_i^2$. Note that this entails that z_i is not included in the training set, corresponding to nonconformity measure definition (12) and the GPR leave-one-out predictive variance (10b). Therefore, a normalized nonconformity measure for GPR-CP can be defined as

$$\alpha_i = \left| \frac{y_i - \hat{y}_i}{\sqrt{\gamma \hat{\sigma}_i^2}} \right|, \quad (19)$$

where the root parameter γ controls the sensitivity of the measure to changes of $\hat{\sigma}_i^2$. The new definitions of **a** and **b** can be obtained by dividing each a_i and b_i in (14) by

$$\sqrt{\frac{1}{[(K + \sigma_n^2 I)^{-1}]_{ii}}}, \quad (20)$$

Specifically,

$$\mathbf{a} = (K + \sigma_n^2 I)^{-1} \mathbf{y}_{\mathbf{a}} / \text{diag}((K + \sigma_n^2 I)^{-1})^{1-\frac{1}{\gamma}}, \quad (21a)$$

$$\mathbf{b} = (K + \sigma_n^2 I)^{-1} \mathbf{y}_{\mathbf{b}} / \text{diag}((K + \sigma_n^2 I)^{-1})^{1-\frac{1}{\gamma}}, \quad (21b)$$

where \mathbf{v}^p corresponds to raising each element of vector \mathbf{v} to the power p .

Note that this nonconformity measure includes both nonconformity measures (11) and (12) as special cases when $\gamma = 1$ and $\gamma = \infty$ respectively. To see this compare the definitions of **a** and **b** in (21) with those in (13) and (14). When $\gamma = 1$ there is a small difference between (21) and (13), namely the multiplication of all nonconformity scores by σ_n^2 in (13). This however, does not change the resulting p-values and PIs since the points where $a_i(\tilde{y}) = a_{l+1}(\tilde{y})$ for $i = 1, \dots, l$ remain exactly the same.

5 EXPERIMENTAL EVALUATION

This Section begins with an assessment of the performance of the proposed approach and the original GPR technique on artificial data, considering two scenarios: one where the exact model hyperparameters are known and one where the hyperparameters are unknown. Subsequently, it evaluates GPR-CP using four benchmark data sets from the UCI Machine Learning repository [52]. This evaluation includes comparisons with the original GPR technique, four recently proposed recalibration techniques [47]–[49], [51] and two existing transductive CPs [14], [17].

The implementations of both GPR and GPR-CP are based on the GPML Matlab code developed by Carl Edward Rasmussen and Hannes Nickisch, available on the website of [6]. Additionally, the implementations of the four recalibration techniques are based on the TorchUQ [49] and Crepes [53] Python libraries as well as the code accompanying [48].

5.1 Evaluation Metrics

As the aim of this work is the provision of PIs, the evaluation is centered on their calibration and tightness, at the confidence levels of 90%, 95% and 99%. Calibration is assessed by examining whether the empirical miscoverage rate of the PIs matches the nominal miscoverage rate (one minus the required confidence level). This is in effect the guarantee provided by CP, see Theorem 1. Tightness is assessed by the mean width of the PIs. Narrower PIs are more precise, provided they align with the expected miscoverage rates. Significantly exceeding the nominal miscoverage rate marks a critical shortfall, indicating unreliable PIs, regardless of how tight they are.

It's important to highlight that recalibration techniques are commonly assessed based on their sharpness, with metrics such as the Negative Log Likelihood (NLL) and Continuous Ranked Probability Score (CRPS), and their calibration, using metrics like the Expected Calibration Error (ECE). As these metrics are not directly applicable to PIs, the comparison performed concentrates on the PIs derived from the outputs of recalibration techniques at the specified confidence levels.

5.2 Artificial Data

The first set of experiments compares the PIs produced by the proposed approach and the original GPR technique (based on the output variance for each instance) on artificially generated data when the model is well-specified.

Ten data sets were generated consisting of 500 training and 1000 test observations with inputs drawn randomly from a standard Gaussian distribution. The outputs of each data set were generated as $y_i = f(x_i) + \epsilon$, where ϵ is Gaussian noise $\mathcal{N}(\epsilon|0, \sigma_n^2)$ with $\sigma_n = 0.1$ and f is a Gaussian Process with a zero mean function and a squared exponential (SE) covariance function with covariance hyperparameters $(l, \sigma_f) = (1, 1)$; i.e. a unit length scale and a unit signal magnitude. The same mean function, covariance function and hyperparameters were used for the application of the two methods on these data sets. GPR-CP utilized the normalized nonconformity measure (19), corresponding to

Method	γ	Mean PI Width			Miscoverage (%)		
		90%	95%	99%	90%	95%	99%
GPR		1.219	1.453	1.909	10.27	4.90	1.02
GPR-CP	1	2.360	3.167	4.823	10.60	4.73	0.91
	2	<u>1.211</u>	<u>1.442</u>	<u>1.905</u>	10.51	5.14	1.09
	∞	1.377	1.853	2.953	9.88	5.04	1.06

TABLE 1

Comparison of the proposed approach and the original GPR on artificial data when the model is well-specified (the smallest PI widths appear in bold and underlined).

Method	γ	Mean PI Width			Miscoverage (%)		
		90%	95%	99%	90%	95%	99%
GPR		1.834	2.185	2.872	8.51	5.21	2.59
GPR-CP	1	1.935	2.595	5.162	10.25	4.74	1.00
	2	<u>1.716</u>	<u>2.259</u>	<u>3.866</u>	10.29	4.78	1.03
	∞	1.875	2.532	4.092	10.45	5.09	0.99

TABLE 2

Comparison of the proposed approach and the original GPR on artificial data with outliers and unknown hyperparameters (the smallest PI widths of GPR-CP appear in bold and underlined).

the vectors \mathbf{a} and \mathbf{b} defined in (21), with γ set to 1, 2 and ∞ ; recall that the first and last of these values of γ are equivalent to definitions (11) and (12) respectively.

Table 1 reports the mean width of the PIs produced by each method for all ten data sets together with the corresponding miscoverage percentages. In this case the PIs produced by both methods are well-calibrated, as their miscoverage rates are very close to the required significance levels. In terms of PI tightness, the smallest widths of GPR-CP are obtained with the normalized version of the nonconformity measure (i.e. $\gamma = 2$) and are slightly smaller than those obtained by the original GPR technique.

A second set of experiments was performed on the same type of data, however this time with probability 0.1 “outlier” observations were generated, for which the noise standard deviation was 1 instead of 0.1. Again ten data sets were generated consisting of 500 training and 1000 test observations. Additionally, the zero mean function and SE covariance function that were used for generating the data were also used for the application of the two methods on these data sets. In this case though, the hyperparameters (length scale, signal magnitude and noise standard deviation) were optimized by minimizing the negative log marginal likelihood.

Table 2 reports the results of the proposed approach and the original GPR technique on these data sets. Although the miscoverage rates of the PIs produced by the original GPR technique for the 90% and 95% confidence levels are again near or below the required significance levels, that of the 99% confidence level is more than double the required level. This demonstrates experimentally that when the GPR model is not well-specified, which is typically the case for real data, the resulting PIs become misleading. On the contrary, the corresponding miscoverage rates of the proposed approach are again in all cases very close to the required levels. In terms of PI tightness, the normalized version of the nonconformity measure ($\gamma = 2$) again gave the smallest widths of

Method	Covariance Function	γ	Boston Housing						Auto-mpg					
			Mean PI Width			Miscoverage (%)			Mean PI Width			Miscoverage (%)		
			90%	95%	99%	90%	95%	99%	90%	95%	99%	90%	95%	99%
GPR	SE		9.230	10.997	14.453	8.02	5.02	2.69	8.307	9.898	13.009	8.49	5.28	2.68
	RQ		9.146	10.897	14.322	8.14	5.32	2.79	8.299	9.888	12.995	8.55	5.36	2.70
	NN		9.031	10.760	14.142	8.66	5.40	2.67	8.276	9.861	12.960	8.57	5.28	2.70
	Matern (3/2)		9.093	10.834	14.239	7.83	5.38	2.87	8.297	9.886	12.993	8.67	5.48	2.60
	Matern (5/2)		9.116	10.862	14.276	8.08	5.26	2.77	8.298	9.887	12.994	8.65	5.41	2.68
GPR-RI	SE		9.369	12.451	20.547	11.64	5.51	1.78	8.454	11.506	19.420	11.12	6.35	1.71
GPR-RB	SE		9.137	11.469	16.788	11.01	6.62	2.41	8.134	10.208	14.898	11.71	6.53	1.86
GPR-RM	SE		9.457	12.133	20.471	11.17	5.63	2.17	8.489	10.954	18.440	10.99	5.79	1.86
GPR-RC *	SE		10.372	16.205	∞	9.01	3.52	0.00	9.710	13.188	∞	8.93	4.54	0.00
RR-CP *	SE		11.651	15.042	27.074	9.86	4.72	0.83	8.015	10.235	20.696	9.80	4.92	0.84
kNNR-CP *			11.592	15.300	25.721	9.76	4.90	0.89	8.521	11.587	21.383	9.57	4.90	0.84
GPR-CP *	SE	1	9.678	12.978	23.197	10.36	4.84	0.87	7.801	10.302	19.321	10.36	4.87	0.82
		2	8.277	11.078	19.773	10.53	4.94	0.91	7.746	10.286	19.315	10.20	4.87	0.82
		3	8.140	10.671	19.106	10.87	4.98	1.13	7.737	10.300	19.349	10.10	4.97	0.82
		4	8.149	10.589	19.978	11.23	5.16	0.95	7.745	10.303	19.379	10.18	4.97	0.82
		8	8.282	<u>10.659</u>	20.584	11.25	5.47	1.03	7.761	10.315	19.471	10.23	4.97	0.87
		∞	8.468	10.938	22.192	11.03	5.51	0.91	7.777	10.341	19.687	10.23	5.00	0.87
GPR-CP *	RQ	1	9.878	13.391	24.248	10.34	4.94	0.97	7.812	10.275	19.256	10.46	5.08	0.84
		2	8.212	11.197	20.147	10.53	4.96	1.03	7.749	10.273	19.270	10.31	5.03	0.87
		∞	8.368	10.845	23.501	11.01	5.55	0.95	7.778	10.369	19.685	10.33	5.03	0.87
GPR-CP *	NN	1	9.528	12.863	21.461	10.22	4.80	0.95	7.794	10.049	18.984	10.41	5.13	0.82
		2	8.273	11.029	19.533	10.61	5.10	0.91	7.769	10.013	18.920	10.46	5.08	0.82
		∞	8.349	11.031	22.270	10.51	5.18	0.91	7.855	10.080	19.063	10.56	5.03	0.92
GPR-CP *	Matern (3/2)	1	9.797	13.474	24.718	10.18	4.84	0.87	7.874	10.283	18.932	10.13	5.08	0.82
		2	8.144	11.306	20.239	10.32	4.86	1.01	7.764	10.374	19.017	10.33	5.03	0.82
		∞	8.247	10.712	24.463	10.89	5.34	0.87	7.793	10.565	19.681	10.28	5.03	0.87
GPR-CP *	Matern (5/2)	1	9.858	13.375	24.173	10.20	4.82	0.95	7.880	10.245	19.100	10.15	5.10	0.82
		2	8.159	11.206	20.040	10.45	4.88	1.03	7.770	10.313	19.156	10.28	5.08	0.82
		∞	8.342	10.820	23.506	10.99	5.45	0.95	7.767	10.440	19.708	10.41	4.92	0.87

TABLE 3

Results of all approaches on the Boston Housing and Auto-mpg data sets (* indicates the approaches that produce well-calibrated PIs across all confidence levels; the best mean PI widths over well-calibrated approaches appear in bold and underlined).

GPR-CP, which are smaller than the ones produced by the original GPR technique for the 90% confidence level and quite close to those produced by the original GPR for the 95% confidence level.

5.3 Benchmark Data

The performance of the proposed approach was evaluated on four benchmark data sets from the UCI Machine Learning repository [52]:

- *Boston Housing*, which lists the median house prices for 506 different areas of Boston MA in \$1000s. Each area is described by 13 inputs such as pollution and crime rate.
- *Auto-mpg*, which concerns fuel consumption in miles per gallon (mpg). The original data set consisted of 398 observations out of which 6 were missing input values and were discarded. Furthermore, one input was also discarded as it was a unique identifying string. The remaining data set had 7 inputs such as engine capacity and number of cylinders.
- *CPU Performance* (or Machine), which lists the relative performance of 209 CPUs based on six continuous inputs and 1 multi-valued discrete input (the vendor).

- *Servo*, which is concerned with the rise time of a servo mechanism in terms of two continuous gain settings and two discrete choices of mechanical link-ages. It consists of 167 observations.

All experiments consisted of 10 random runs of a 10-fold cross-validation process for each data set. The inputs were normalized by setting their mean to 0 and their standard deviation to 1 based on the training examples of each fold.

The proposed approach and original GPR technique were extensively evaluated using 5 covariance functions: Squared Exponential (SE), Rational Quadratic (RQ), Neural Network (NN) and Matern with smoothness set to $\nu = 3/2$ and $\nu = 5/2$. In all cases, hyperparameters were optimized within each training set by minimizing the negative log marginal likelihood. To mitigate the risk of converging to local minima, the minimization process was performed 3 times with different random initial values and the hyperparameters that resulted in the lowest negative log marginal likelihood were selected. It's worth noting that exactly the same hyperparameters were used for both methods.

The covariance functions that gave the smallest mean negative log marginal likelihood over all runs and folds for each data set were: Matern with $\nu = 3/2$ for Boston Housing, Rational Quadratic for Auto-mpg, Neural Network for CPU Performance, and Matern with $\nu = 5/2$ for Servo.

Method	Covariance Function	γ	CPU Performance						Servo					
			Mean PI Width			Miscoverage (%)			Mean PI Width			Miscoverage (%)		
			90%	95%	99%	90%	95%	99%	90%	95%	99%	90%	95%	99%
GPR	SE		108.78	129.61	170.34	12.58	9.33	5.55	1.853	2.208	2.902	9.04	7.01	4.67
	RQ		111.12	132.40	174.02	12.15	9.14	5.55	1.823	2.172	2.854	9.82	7.72	4.67
	NN		100.52	119.77	157.41	13.54	9.43	5.41	1.951	2.324	3.054	7.90	6.23	3.83
	Matern (3/2)		108.34	129.09	169.66	11.53	8.66	5.45	1.801	2.146	2.821	8.74	7.07	4.91
	Matern (5/2)		107.75	128.39	168.74	12.01	8.61	5.60	1.810	2.157	2.835	9.34	7.01	4.97
GPR-RI	SE		133.93	182.25	285.59	11.87	6.79	2.25	1.919	2.772	4.383	11.38	6.95	3.59
GPR-RB	SE		104.65	131.84	∞	13.35	8.04	3.16	1.348	∞	∞	9.22	5.81	2.93
GPR-RM	SE		137.75	191.82	279.07	12.39	7.75	3.06	1.902	2.639	4.133	11.14	7.01	3.77
GPR-RC *	SE		165.19	228.18	∞	9.67	4.55	0.00	3.701	∞	∞	4.73	0.00	0.00
RR-CP *	SE		∞	∞	∞	9.90	4.64	0.57	1.869	2.945	7.224	9.76	4.31	0.60
k NNR-CP *	SE		141.57	206.03	545.31	9.38	4.55	0.62	1.423	3.023	7.675	10.42	4.55	0.60
GPR-CP *	SE	1	160.57	221.37	333.62	10.57	5.79	1.05	1.731	2.989	6.171	10.36	4.55	0.54
		2	110.33	165.04	253.38	10.96	5.17	1.05	1.650	2.872	6.699	10.24	4.55	0.66
		3	106.65	157.14	295.21	11.77	5.89	0.77	1.631	2.846	6.908	10.36	4.55	0.66
		4	109.79	154.14	332.34	11.48	6.08	0.91	1.623	2.833	7.018	10.36	4.55	0.66
		8	115.18	158.23	414.94	10.91	6.08	1.15	1.614	2.814	7.191	10.42	4.49	0.66
		∞	121.52	176.86	537.25	10.57	5.55	1.24	1.609	2.798	7.372	10.36	4.43	0.66
GPR-CP *	RQ	1	161.34	228.68	389.69	10.86	5.55	1.05	1.720	3.001	6.018	11.02	4.79	0.78
		2	115.72	177.96	316.22	11.05	5.12	0.86	1.614	2.875	6.489	11.14	4.55	0.66
		∞	125.71	188.65	551.74	11.10	5.45	1.20	1.574	2.782	7.129	11.02	4.67	0.66
GPR-CP *	NN	1	139.70	191.58	∞	10.77	5.98	0.91	1.688	2.909	7.314	9.70	4.25	0.66
		2	109.35	156.70	277.73	10.91	5.41	1.10	1.650	2.835	7.628	9.76	4.31	0.60
		∞	116.16	164.20	∞	11.29	5.31	0.77	1.625	2.772	7.997	9.88	4.37	0.60
GPR-CP *	Matern (3/2)	1	148.93	222.75	392.61	10.43	5.26	0.81	1.774	3.109	5.832	9.82	4.55	0.72
		2	111.93	180.24	316.88	10.57	4.78	0.77	1.632	2.951	6.280	9.82	4.37	0.54
		∞	124.25	189.81	523.97	10.57	5.26	0.96	1.550	2.835	6.915	9.64	4.61	0.60
GPR-CP *	Matern (5/2)	1	160.58	228.93	386.71	10.48	5.50	0.91	1.769	3.062	5.907	10.06	4.55	0.78
		2	112.22	177.38	305.51	10.81	5.22	0.91	1.650	2.920	6.376	10.12	4.37	0.60
		∞	124.00	188.27	532.02	10.81	5.41	1.10	1.569	2.817	7.021	10.00	4.61	0.66

TABLE 4

Results of all approaches on the CPU Performance and Servo data sets (* indicates the approaches that produce well-calibrated PIs across all confidence levels; the best mean PI widths over well-calibrated approaches appear in bold and underlined).

GPR-CP utilized the normalized nonconformity measure (19), corresponding to the vectors \mathbf{a} and \mathbf{b} defined in (21). The nonconformity measure parameter γ was set to 1, 2 and ∞ in all experiments. Additionally, to further explore its impact on the results it was also set to 3, 4 and 8 when utilizing the SE covariance function.

For comparison with previously proposed techniques, the same experiments were conducted with four recalibration approaches and two existing transductive CP approaches. All four recalibration approaches employed GPR with the SE covariance function as underlying technique, utilizing the Scikit-learn [54] implementation of GPR. The number of instances withheld for the calibration process was set to 25% of the training set (following [49]). It's worth noting that not employing a separate calibration set, as suggested in [47] and [48], resulted in extremely uncalibrated PIs and was therefore not considered as an option.

The specific recalibration approaches considered are:

- Isotonic Calibration (GPR-RI): Algorithm 1 in [47] with isotonic regression as recalibrator.
- GP-BETA Calibration (GPR-RB): Algorithm proposed in [48] with the number of inducing points set to 64.
- Modular Conformal Calibration (GPR-RM): Algorithm 1 in [49] with the Neural Autoregressive Flow

(NAF) interpolation algorithm.

- Split Conformal Predictive System (GPR-RC): Algorithm 1 in [51].

The same experiments were conducted with two existing transductive CPs: the Ridge Regression CP (RR-CP) [14] and the k -Nearest Neighbours Regression CP (k NNR-CP) [17]. As mentioned in Section 2.2, RR-CP uses the standard (non-normalized) regression nonconformity measure, while k NNR-CP is the only existing TCP approach that employs a normalized measure.

RR-CP utilized an RBF kernel, which corresponds to the SE covariance function of GPR. The kernel parameter and ridge factor were optimized by minimizing the leave-one-out error on each fold using the gradient descent approach proposed in [55] and the corresponding code provided online². The parameter k of nearest neighbours for k NNR-CP was selected by performing a 10-fold cross-validation process with the original k -NNR technique on the whole of each data set and selecting the value of k that gave the smallest error. The use of the whole data set involves snooping, but this is in favour of k NNR-CP.

Tables 3 and 4 present the results of all approaches on the Boston Housing and Auto-mpg, and on the CPU

2. The code is located at <http://olivier.chapelle.cc/ams/>

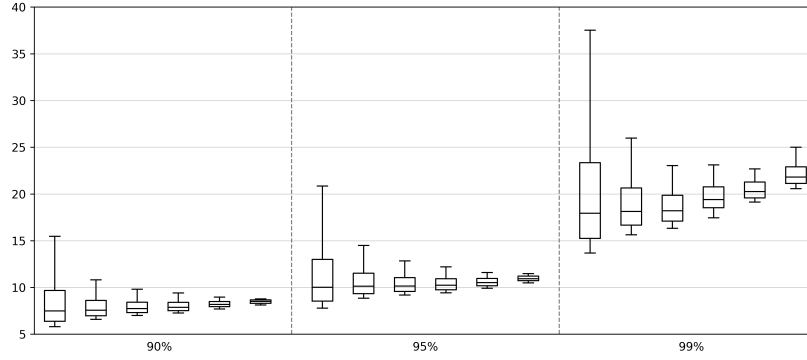


Fig. 2. Boston Housing data set PI width distribution for the 90%, 95% and 99% confidence levels (Each part contains the boxplots for the PI widths produced with γ set to 1, 2, 3, 4, 8 and ∞ from left to right).

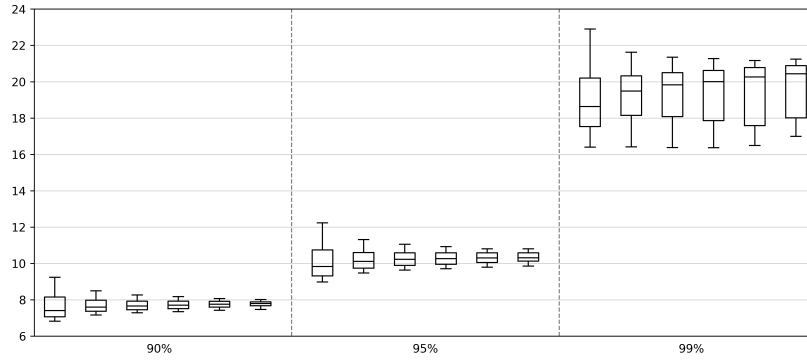


Fig. 3. Auto-mpg data set PI width distribution for the 90%, 95% and 99% confidence levels (Each part contains the boxplots for the PI widths produced with γ set to 1, 2, 3, 4, 8 and ∞ from left to right).

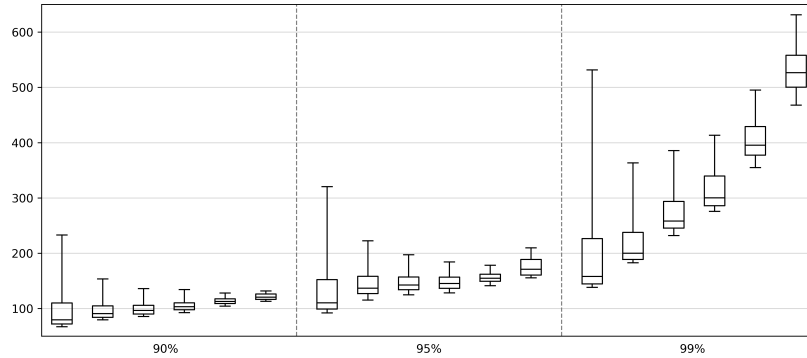


Fig. 4. CPU Performance data set PI width distribution for the 90%, 95% and 99% confidence levels (Each part contains the boxplots for the PI widths produced with γ set to 1, 2, 3, 4, 8 and ∞ from left to right).

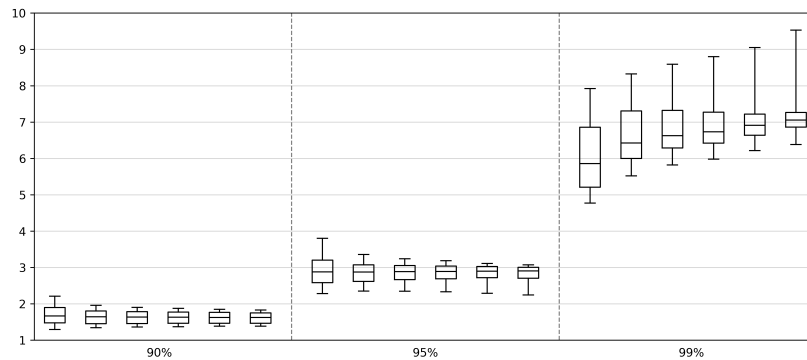


Fig. 5. Servo data set PI width distribution for the 90%, 95% and 99% confidence levels (Each part contains the boxplots for the PI widths produced with γ set to 1, 2, 3, 4, 8 and ∞ from left to right).

Performance and Servo data sets, respectively. Specifically, these tables present the mean PI widths together with the miscoverage percentage of the corresponding PIs for each confidence level. For ease of presentation, the approaches are divided into 8 groups consisting of the original GPR with the 5 covariance functions, the four recalibration approaches, the two existing TCP approaches, and one group for the proposed approach with each of the 5 covariance functions.

By assessing the well-calibratedness of approaches one can observe that the PIs of the original GPR, GPR-RI, GPR-RB and GPR-RM approaches can become very misleading. Across all data sets, these approaches fail to cover the true label in significantly more than the required 1% of cases at the 99% confidence level. Moreover, for the CPU Performance and Servo data sets, the considerably higher than the nominal miscoverage percentages extend to the 95% confidence level, and in some cases, even to the 90% confidence level. On the contrary, the miscoverage rates of the PIs produced by the proposed approach as well as GPR-RC, RR-CP and k NNR-CP are close to the required significance levels in all cases. It is important to note here that the well-calibratedness of the proposed approach is not affected by the choice of covariance function or nonconformity measure.

In assessing PI tightness, the best mean PI widths among the four well-calibrated approaches are marked in bold and underlined. In nearly all cases GPR-CP produces the tightest mean PI widths. The sole exception is observed at the 90% confidence level for the Servo data set.

When comparing GPR-CP with SE covariance and $\gamma = 2$ to the four recalibration approaches, one can notice that in virtually all cases, either the mean PI widths of GPR-CP are tighter, or the corresponding PIs have an extremely high miscoverage percentage, surpassing 30% above the significance level. Once again the only exception is at the 90% confidence level for the Servo data set.

Performing the same comparison with the two existing TCP approaches shows that the mean PI widths of GPR-CP are again almost always better. There are only two exceptions: RR-CP gives slightly smaller widths for the 95% confidence level on the Auto-mpg data set, and k NNR-CP gives smaller widths for the 90% confidence level on the Servo data set. Another important observation in these results is the sensitivity of the non-normalized nonconformity measure of RR-CP, which can result in some extremely wide intervals. This is particularly evident in the widths produced for the CPU Performance data set, underlining the significant advantage of normalized nonconformity measures.

In fact, the substantial difference that can be observed between the well-calibrated mean widths of all existing (recalibration and CP) approaches and those of GPR-CP on the Boston Housing and CPU Performance data sets demonstrates the superiority of GPR-CP when combined with the normalized nonconformity measure proposed in this work.

Figures 2-5 complement the information in Tables 3 and 4 by displaying boxplots of the PI widths generated by GPR-CP with SE covariance for each data set. In particular, each boxplot shows the median, upper and lower quartiles, and

upper and lower deciles of the corresponding PI widths. Each plot is divided into three sections corresponding to the three confidence levels of interest (90%, 95% and 99%) and each section contains the boxplots for the PI widths produced with γ set to 1, 2, 3, 4, 8, and ∞ arranged from left to right.

A comparison of the results obtained with the different values of γ , firstly demonstrates the substantial positive impact of the normalized nonconformity measure on the tightness of the resulting PIs. This is evident from the PIs generated when γ is set to ∞ , which disregards the variance of observations. These PIs have the largest median widths across almost all cases. Notably, for the Boston Housing and CPU Performance data sets the large majority of the PIs produced with $\gamma = \infty$ are wider than the median width obtained with all other γ values. The most pronounced difference can be observed in Figure 4 at the 99% confidence level, where the lower decile of the widths obtained with $\gamma = \infty$ surpasses the upper deciles of the widths obtained with γ values of 2, 3 and 4.

Conversely, when γ is set to 1 the median interval width is typically the smallest. However, this setting appears to result in an overly sensitive nonconformity measure, leading to some exceptionally wide PIs and, consequently, much larger mean widths, which are in many cases even larger than those produced with $\gamma = \infty$.

Increasing γ reduces the sensitivity of the measure, leading to a decrease in the variability of PI widths, which is typically much higher above the median, and an increase in the median itself. Initially, the impact of the sensitivity reduction to the variability of the widths is more significant than the increase to their median value, resulting in, on average, tighter PIs. As γ continues increasing, the effect of the variability reduction becomes less significant compared to the increase in the median, causing the mean PI widths to start expanding. Overall, the choice of γ is dependent on the specific data set, with values in the range of 2 to 4 often resulting in the optimal balance for PI widths.

6 CONCLUSION

This work developed a transductive Conformal Predictor based on the popular Gaussian Process Regression technique and defined a normalized nonconformity measure based on the variance produced by GPR. The resulting approach retains all the desirable properties of GPR and guarantees well-calibrated PIs without assuming anything more than exchangeability of the data, as opposed to the much stronger assumptions of conventional GPR.

The presented experimental results highlight the superiority of the PIs generated by the proposed GPR-CP in comparison to existing approaches. In terms of calibration, the PIs of the original GPR and three of the four recalibration methods considered often exhibit much higher miscoverage rates than the corresponding significance level, rendering them potentially misleading. In contrast, GPR-CP consistently produces well-calibrated PIs regardless of the particular model and data characteristics. Concerning PI tightness, GPR-CP outperforms all other methods, with a substantial difference in mean widths on two of the four

data sets, demonstrating the significant advantage of the proposed normalized nonconformity measure.

Immediate future directions of this work include the development of a GPR-CP variant based on sparse GP approaches (see e.g. [56]), that will enable the computationally efficient processing of large data sets. Additionally, further research will explore the development of new normalized nonconformity measures for regression CP, aiming at producing even tighter PIs.

ACKNOWLEDGMENT

The author is grateful to Professors V. Vovk and A. Gammerman for useful discussions.

REFERENCES

- [1] M. P. Deisenroth, D. Fox, and C. E. Rasmussen, "Gaussian processes for data-efficient learning in robotics and control," *IEEE Transactions on Pattern Analysis and Machine Intelligence*, vol. 37, no. 2, pp. 408–423, 2015.
- [2] D. Nguyen-Tuong and J. Peters, "Incremental online sparsification for model learning in real-time robot control," *Neurocomputing*, vol. 74, no. 11, pp. 1859–1867, 2011, adaptive Incremental Learning in Neural Networks Learning Algorithm and Mathematic Modelling Selected papers from the International Conference on Neural Information Processing 2009 (ICONIP 2009). [Online]. Available: <https://www.sciencedirect.com/science/article/pii/S0925231211000701>
- [3] A. Kendall, J. Hawke, D. Janz, P. Mazur, D. Reda, J.-M. Allen, V.-D. Lam, A. Bewley, and A. Shah, "Learning to drive in a day," in *2019 International Conference on Robotics and Automation (ICRA)*, 2019, pp. 8248–8254.
- [4] F. Berkenkamp, M. Turchetta, A. P. Schoellig, and A. Krause, "Safe model-based reinforcement learning with stability guarantees," in *Proceedings of the 31st International Conference on Neural Information Processing Systems (NIPS 2017)*, 2017, pp. 908–919.
- [5] H. Soleimani, J. Hensman, and S. Saria, "Scalable joint models for reliable uncertainty-aware event prediction," *IEEE Transactions on Pattern Analysis and Machine Intelligence*, vol. 40, no. 8, pp. 1948–1963, 2018.
- [6] C. E. Rasmussen and C. K. I. Williams, *Gaussian Processes for Machine Learning*. MIT Press, 2006.
- [7] N. Srinivas, A. Krause, S. M. Kakade, and M. W. Seeger, "Information-theoretic regret bounds for gaussian process optimization in the bandit setting," *IEEE Transactions on Information Theory*, vol. 58, no. 5, pp. 3250–3265, 2012.
- [8] S. R. Chowdhury and A. Gopalan, "On kernelized multi-armed bandits," *CoRR*, vol. abs/1704.00445, 2017. [Online]. Available: <http://arxiv.org/abs/1704.00445>
- [9] A. Capone, A. Lederer, and S. Hirche, "Gaussian process uniform error bounds with unknown hyperparameters for safety-critical applications," in *Proceedings of the 39th International Conference on Machine Learning*, ser. Proceedings of Machine Learning Research, K. Chaudhuri, S. Jegelka, L. Song, C. Szepesvari, G. Niu, and S. Sabato, Eds., vol. 162. PMLR, 17–23 Jul 2022, pp. 2609–2624. [Online]. Available: <https://proceedings.mlr.press/v162/capone22a.html>
- [10] C. Fiedler, C. W. Scherer, and S. Trimpe, "Practical and rigorous uncertainty bounds for gaussian process regression," in *Proceedings of the AAAI Conference on Artificial Intelligence*, vol. 35, no. 8, May 2021, pp. 7439–7447. [Online]. Available: <https://ojs.aaai.org/index.php/AAAI/article/view/16912>
- [11] V. Vovk, A. Gammerman, and G. Shafer, *Algorithmic Learning in a Random World*, 2nd ed. Springer, 2022.
- [12] A. N. Angelopoulos and S. Bates, "A gentle introduction to conformal prediction and distribution-free uncertainty quantification," 2021. [Online]. Available: <https://arxiv.org/abs/2107.07511>
- [13] H. Papadopoulos, "Cross-conformal prediction with ridge regression," in *Statistical Learning and Data Sciences*, A. Gammerman, V. Vovk, and H. Papadopoulos, Eds. Cham: Springer International Publishing, 2015, pp. 260–270.
- [14] I. Nouretdinov, T. Melliush, and V. Vovk, "Ridge regression confidence machine," in *Proceedings of the 18th International Conference on Machine Learning (ICML'01)*. San Francisco, CA: Morgan Kaufmann, 2001, pp. 385–392.
- [15] J. Lei, "Fast exact conformalization of the lasso using piecewise linear homotopy," *Biometrika*, vol. 106, no. 4, pp. 749–764, 09 2019. [Online]. Available: <https://doi.org/10.1093/biomet/asz046>
- [16] H. Papadopoulos, A. Gammerman, and V. Vovk, "Normalized nonconformity measures for regression conformal prediction," in *Proceedings of the IASTED International Conference on Artificial Intelligence and Applications (AIA 2008)*. ACTA Press, 2008, pp. 64–69.
- [17] H. Papadopoulos, V. Vovk, and A. Gammerman, "Regression conformal prediction with nearest neighbours," *Journal of Artificial Intelligence Research*, vol. 40, pp. 815–840, 2011. [Online]. Available: <http://dx.doi.org/10.1613/jair.3198>
- [18] A. Gammerman, V. Vapnik, and V. Vovk, "Learning by transduction," in *Proceedings of the Fourteenth Conference on Uncertainty in Artificial Intelligence*. San Francisco, CA: Morgan Kaufmann, 1998, pp. 148–156.
- [19] C. Saunders, A. Gammerman, and V. Vovk, "Transduction with confidence and credibility," in *Proceedings of the 16th International Joint Conference on Artificial Intelligence*, vol. 2. Los Altos, CA: Morgan Kaufmann, 1999, pp. 722–726.
- [20] K. Proedrou, I. Nouretdinov, V. Vovk, and A. Gammerman, "Transductive confidence machines for pattern recognition," in *Proceedings of the 13th European Conference on Machine Learning (ECML'02)*, ser. LNCS, vol. 2430. Springer, 2002, pp. 381–390.
- [21] H. Papadopoulos, V. Vovk, and A. Gammerman, "Qualified predictions for large data sets in the case of pattern recognition," in *Proceedings of the 2002 International Conference on Machine Learning and Applications (ICMLA'02)*. CSREA Press, 2002, pp. 159–163.
- [22] H. Papadopoulos, "Inductive Conformal Prediction: Theory and application to neural networks," in *Tools in Artificial Intelligence*, P. Fritzsche, Ed. Vienna, Austria: InTech, 2008, ch. 18, pp. 315–330. [Online]. Available: <http://dx.doi.org/10.5772/6078>
- [23] U. Johansson, H. Boström, and T. Löfström, "Conformal prediction using decision trees," in *2013 IEEE 13th International Conference on Data Mining*, 2013, pp. 330–339.
- [24] D. Devetyarov and I. Nouretdinov, "Prediction with confidence based on a random forest classifier," in *Artificial Intelligence Applications and Innovations*, H. Papadopoulos, A. S. Andreou, and M. Bramer, Eds. Berlin, Heidelberg: Springer Berlin Heidelberg, 2010, pp. 37–44.
- [25] A. Lambrou, H. Papadopoulos, and A. Gammerman, "Reliable confidence measures for medical diagnosis with evolutionary algorithms," *IEEE Transactions on Information Technology in Biomedicine*, vol. 15, no. 1, pp. 93–99, 2011.
- [26] H. Papadopoulos, K. Proedrou, V. Vovk, and A. Gammerman, "Inductive confidence machines for regression," in *Proceedings of the 13th European Conference on Machine Learning (ECML'02)*, ser. LNCS, vol. 2430. Springer, 2002, pp. 345–356.
- [27] H. Papadopoulos and H. Haralambous, "Reliable prediction intervals with regression neural networks," *Neural Networks*, 2011. [Online]. Available: <http://dx.doi.org/10.1016/j.neunet.2011.05.008>
- [28] U. Johansson, H. Boström, T. Löfström, and H. Linusson, "Regression conformal prediction with random forests," *Machine Learning*, vol. 97, pp. 155–176, 2014.
- [29] H. Boström, H. Linusson, T. Löfström, and U. Johansson, "Accelerating difficulty estimation for conformal regression forests," *Annals of Mathematics and Artificial Intelligence*, vol. 81, no. 1, pp. 125–144, 2017.
- [30] U. Johansson, H. Boström, and T. Löfström, "Investigating normalized conformal regressors," in *2021 IEEE Symposium Series on Computational Intelligence (SSCI)*, 2021, pp. 01–08.
- [31] A. Gammerman, V. Vovk, B. Burford, I. Nouretdinov, Z. Luo, A. Chervonenkis, M. Waterfield, R. Cramer, P. Tempst, J. Villanueva, M. Kabir, S. Camuzeaux, J. Timms, U. Menon, and I. Jacobs, "Serum proteomic abnormality predating screen detection of ovarian cancer," *The Computer Journal*, vol. 52, no. 3, pp. 326–333, 2009.
- [32] H. Papadopoulos, E. Kyriacou, and A. Nicolaidis, "Unbiased confidence measures for stroke risk estimation based on ultrasound carotid image analysis," *Neural Computing and Applications*, vol. 28, no. 6, pp. 1209–1223, 2017.

- [33] M. Eklund, U. Norinder, S. Boyer, and L. Carlsson, "The application of conformal prediction to the drug discovery process," *Annals of Mathematics and Artificial Intelligence*, vol. 74, pp. 117–132, 2015.
- [34] F. Svensson, N. Aniceto, U. Norinder, I. Cortes-Ciriano, O. Spjuth, L. Carlsson, and A. Bender, "Conformal regression for quantitative structure-activity relationship modeling—quantifying prediction uncertainty," *Journal of Chemical Information and Modeling*, vol. 58, no. 5, pp. 1132–1140, 2018.
- [35] C. Kath and F. Ziel, "Conformal prediction interval estimation and applications to day-ahead and intraday power markets," *International Journal of Forecasting*, vol. 37, no. 2, pp. 777–799, 2021. [Online]. Available: <https://www.sciencedirect.com/science/article/pii/S0169207020301473>
- [36] H. Papadopoulos, E. Papatheochous, and A. S. Andreou, "Reliable confidence intervals for software effort estimation," in *Proceedings of the 2nd Workshop on Artificial Intelligence Techniques in Software Engineering (AISEW 2009)*, ser. CEUR Workshop Proceedings, vol. 475. CEUR-WS.org, 2009. [Online]. Available: ceur-ws.org/Vol-475/AISEW2009/22-pp-211-220-208.pdf
- [37] L. Maltoudoglou, A. Paisios, L. Lenc, J. Martínek, P. Král, and H. Papadopoulos, "Well-calibrated confidence measures for multi-label text classification with a large number of labels," *Pattern Recognition*, vol. 122, p. 108271, 2022.
- [38] A. Lambrou and H. Papadopoulos, "Binary relevance multi-label conformal predictor," in *Conformal and Probabilistic Prediction with Applications*, A. Gammerman, Z. Luo, J. Vega, and V. Vovk, Eds. Cham: Springer International Publishing, 2016, pp. 90–104.
- [39] H. Papadopoulos, "A cross-conformal predictor for multi-label classification," in *Artificial Intelligence Applications and Innovations*, L. Iliadis, I. Maglogiannis, H. Papadopoulos, S. Sioutas, and C. Makris, Eds. Berlin, Heidelberg: Springer Berlin Heidelberg, 2014, pp. 241–250.
- [40] S. Messoudi, S. Destercke, and S. Rousseau, "Ellipsoidal conformal inference for multi-target regression," in *Proceedings of the Eleventh Symposium on Conformal and Probabilistic Prediction with Applications*, ser. Proceedings of Machine Learning Research, U. Johansson, H. Boström, K. An Nguyen, Z. Luo, and L. Carlsson, Eds., vol. 179. PMLR, 24–26 Aug 2022, pp. 294–306. [Online]. Available: <https://proceedings.mlr.press/v179/messoudi22a.html>
- [41] S. Ho and H. Wechsler, "A martingale framework for detecting changes in data streams by testing exchangeability," *IEEE Transactions on Pattern Analysis and Machine Intelligence*, vol. 32, no. 12, pp. 2113–2127, 2010.
- [42] C. Eliades and H. Papadopoulos, "A betting function for addressing concept drift with conformal martingales," in *Proceedings of the Eleventh Symposium on Conformal and Probabilistic Prediction with Applications*, ser. Proceedings of Machine Learning Research, U. Johansson, H. Boström, K. An Nguyen, Z. Luo, and L. Carlsson, Eds., vol. 179. PMLR, 24–26 Aug 2022, pp. 219–238. [Online]. Available: <https://proceedings.mlr.press/v179/eliades22a.html>
- [43] R. Laxhammar and G. Falkman, "Online learning and sequential anomaly detection in trajectories," *IEEE Transactions on Pattern Analysis and Machine Intelligence*, vol. 36, no. 6, pp. 1158–1173, 2014.
- [44] S. Ho and H. Wechsler, "Transductive confidence machine for active learning," in *IJCNN*, vol. 2, 2003, pp. 1435–1440.
- [45] V. Manokhin, "Awesome conformal prediction," Apr. 2022. [Online]. Available: <https://doi.org/10.5281/zenodo.6467205>
- [46] R. F. Barber, E. J. Candès, A. Ramdas, and R. J. Tibshirani, "Predictive inference with the jackknife+," *The Annals of Statistics*, vol. 49, no. 1, pp. 486 – 507, 2021. [Online]. Available: <https://doi.org/10.1214/20-AOS1965>
- [47] V. Kuleshov, N. Fenner, and S. Ermon, "Accurate uncertainties for deep learning using calibrated regression," in *Proceedings of the 35th International Conference on Machine Learning*, ser. Proceedings of Machine Learning Research, J. Dy and A. Krause, Eds., vol. 80. PMLR, 10–15 Jul 2018, pp. 2796–2804. [Online]. Available: <https://proceedings.mlr.press/v80/kuleshov18a.html>
- [48] H. Song, T. Diethe, M. Kull, and P. Flach, "Distribution calibration for regression," in *Proceedings of the 36th International Conference on Machine Learning*, ser. Proceedings of Machine Learning Research, K. Chaudhuri and R. Salakhutdinov, Eds., vol. 97. PMLR, 09–15 Jun 2019, pp. 5897–5906. [Online]. Available: <https://proceedings.mlr.press/v97/song19a.html>
- [49] C. Marx, S. Zhao, W. Neiswanger, and S. Ermon, "Modular conformal calibration," in *Proceedings of the 39th International Conference on Machine Learning*, ser. Proceedings of Machine Learning Research, K. Chaudhuri, S. Jegelka, L. Song, C. Szepesvari, G. Niu, and S. Sabato, Eds., vol. 162. PMLR, 17–23 Jul 2022, pp. 15180–15195. [Online]. Available: <https://proceedings.mlr.press/v162/marx22a.html>
- [50] V. Vovk, J. Shen, V. Manokhin, and M.-g. Xie, "Nonparametric predictive distributions based on conformal prediction," in *Proceedings of the Sixth Symposium on Conformal and Probabilistic Prediction and Applications*, ser. Proceedings of Machine Learning Research, A. Gammerman, V. Vovk, Z. Luo, and H. Papadopoulos, Eds., vol. 60. PMLR, 13–16 Jun 2017, pp. 82–102. [Online]. Available: <https://proceedings.mlr.press/v60/vovk17a.html>
- [51] V. Vovk, I. Petej, I. Nourtdinov, V. Manokhin, and A. Gammerman, "Computationally efficient versions of conformal predictive distributions," *Neurocomputing*, vol. 397, pp. 292–308, 2020. [Online]. Available: <https://www.sciencedirect.com/science/article/pii/S0925231219316042>
- [52] A. Frank and A. Asuncion, "UCI machine learning repository," Irvine, CA, 2010. [Online]. Available: <http://archive.ics.uci.edu/ml>
- [53] H. Boström, "crepes: a python package for generating conformal regressors and predictive systems," in *Proceedings of the Eleventh Symposium on Conformal and Probabilistic Prediction and Applications*, ser. Proceedings of Machine Learning Research, U. Johansson, H. Boström, K. An Nguyen, Z. Luo, and L. Carlsson, Eds., vol. 179. PMLR, 2022.
- [54] F. Pedregosa, G. Varoquaux, A. Gramfort, V. Michel, B. Thirion, O. Grisel, M. Blondel, P. Prettenhofer, R. Weiss, V. Dubourg, J. Vanderplas, A. Passos, D. Cournapeau, M. Brucher, M. Perrot, and E. Duchesnay, "Scikit-learn: Machine learning in Python," *Journal of Machine Learning Research*, vol. 12, pp. 2825–2830, 2011.
- [55] O. Chapelle, V. Vapnik, O. Bousquet, and S. Mukherjee, "Choosing multiple parameters for support vector machines," *Machine Learning*, vol. 46, 2002.
- [56] Y. Cao, M. A. Brubaker, D. J. Fleet, and A. Hertzmann, "Efficient optimization for sparse gaussian process regression," *IEEE Transactions on Pattern Analysis and Machine Intelligence*, vol. 37, no. 12, pp. 2415–2427, 2015.



Harris Papadopoulos is an Associate Professor at the Department of Electrical Engineering, Computer Engineering and Informatics of Frederick University, where he is heading the Computational Intelligence (COIN) Research Laboratory. He is also a Visiting Fellow of the Computer Learning Research Centre of Royal Holloway, University of London, UK. His research primarily focuses on the development of advanced Machine Learning techniques that provide probabilistically valid uncertainty quantification for each prediction under minimal assumptions, and on their application to a diverse array of challenges in various scientific fields. He has published more than 70 research papers in international refereed journals and conferences and co-edited the book "Measures of Complexity: Festschrift in Honor of Alexey Chervonenkis", Springer, 2015. He has been involved in several funded research projects with a total budget of more than 6M euro, frequently taking the lead as the coordinator and initiator. Direct funding to his Lab over the past five years exceeds 1.5M euro. He served as an Associate Editor of the *Evolving Systems Journal* (Springer) from 2015 to 2018 and as guest editor of seven journal special issues. He also served as one of the main organizers of several international conferences and workshops.